

Effect of extrusion ratio on microstructure and mechanical properties of microwave-sintered magnesium and Mg/Y₂O₃ nanocomposite

K. S. Tun · M. Gupta

Received: 20 February 2008 / Accepted: 11 April 2008 / Published online: 23 April 2008
© Springer Science+Business Media, LLC 2008

Abstract The present study establishes that extrusion ratio has a critical role in enhancing microstructural and mechanical characteristics of commercially pure magnesium and a magnesium-based nanocomposite. The study reveals that the best microstructural and mechanical characteristics can be achieved in a Mg/Y₂O₃ nanocomposite provided it is extruded at a ratio higher than a critical extrusion ratio (19:1). An extrusion ratio at 25:1 is found to be the ratio in the present study which leads to significant enhancement in microstructural characteristics (low porosity and good distribution of particulates) and mechanical properties (microhardness, 0.2% YS and UTS) of a Mg/2 wt.%Y₂O₃ nanocomposite. Results of this study also show very close relationship between microhardness and strengths (0.2% YS and UTS) for both pure magnesium and Mg/Y₂O₃ composite extruded at different extrusion ratios.

Introduction

Magnesium-based materials are excellent candidates for structural applications with a tremendous potential to reduce green house gas emission due to their light weight. These materials have certain limitations such as low elastic modulus and ductility which can be circumvented by the use of composite technology [1, 2]. Commonly, reinforcement is used in particulate form to realize low cost and isotropic

properties. In recent years, several attempts have been made to use different types of particulates (metals and ceramic) and in different length scales [3–12]. Particulate reinforcement in nano length scales, such as alumina and yttria, have shown the potential to increase the combination of tensile strengths and ductility [3, 4, 12]. While there have been a number of studies to tailor the properties of magnesium using different types and amount of reinforcement, there has been no attempt made to study the effect of the level of deformation such as extrusion ratio on the microstructure and tensile properties of commercially pure magnesium and magnesium-based nanocomposites. Limited studies exist only on unreinforced alloys such as AZ31 [13], AZ31B [14], and AZ91 [15], and AZ91/SiC composite with micron-size particulates [15].

Accordingly, the primary aim of the present study was to study the effect of extrusion ratio on the microstructure and tensile properties of powder metallurgy-processed magnesium and magnesium-based nanocomposite. Microwave sintering which has a capability to cut the energy consumption up to 90% was used during the powder metallurgy processing.

Experimental procedures

Materials

In this study, magnesium powder of 98.5% purity [impurities insoluble in hydrochloric acid (<0.05%) and iron (<0.05%)] with a size range of 60–300 μm (Merck, Germany) was used as the matrix material and yttria (Y₂O₃) with a particulate size range of 30–50 nm (Inframat Advanced Materials, USA) was used as the ceramic reinforcement phase.

K. S. Tun · M. Gupta (✉)
Department of Mechanical Engineering, National University of
Singapore, 9 Engineering Drive 1, Singapore 117576, Singapore
e-mail: mpegm@nus.edu.sg

Processing

Monolithic magnesium and magnesium nanocomposite ($\text{Mg}/\text{Y}_2\text{O}_3$) containing 2.0 wt.% (0.7 vol.%) of yttria powder were synthesized using powder metallurgy technique. The synthesis process for $\text{Mg}/\text{Y}_2\text{O}_3$ involved blending pure magnesium powder with nano-sized Y_2O_3 powder in a RETSCH PM-400 mechanical alloying machine at 200 rpm for 1 h. No milling media or process control agents were used during the blending step. The blended powder mixtures of Mg and Y_2O_3 were then cold compacted at a pressure of 97 bars (510 MPa) to form billets of 35-mm diameter and 40-mm height using a 100-ton press. Monolithic magnesium was compacted using the same parameters without blending. The compacted billets were sintered using an innovative hybrid microwave sintering technique [16]. The billets were heated to 640 °C in a 900 W, 2.45 GHz SHARP microwave oven (multimode cavity). Sintered billets were subsequently hot extruded at a temperature of 350 °C using different extrusion ratios of 12:1, 19:1, and 25:1 using a 150-ton hydraulic press. As-sintered billets were soaked at 400 °C for 1 h before extrusion.

Density measurements

The density of the extruded Mg and Mg nanocomposites, in a polished condition, was measured using Archimedes' principle. Three samples were randomly selected from extruded rods and were weighed in air and when immersed in distilled water. An A&D ER-182A electronic balance with an accuracy of 0.0001 g was used for recording the weights. The theoretical density of the $\text{Mg}/\text{Y}_2\text{O}_3$ composite was calculated using rule-of-mixture principle, and used to determine the amount of porosity in each case. For this purpose, densities of 1.74 and 5.03 g/cm³ were taken for magnesium and yttria, respectively.

Microstructural characterization

Microstructural characterization studies were conducted to determine grain size, grain morphology, and distribution of reinforcement. HITACHI S-4300 Field Emission Scanning Electron Microscope (FESEM), OLYMPUS metallographic optical microscope, and Scion Image Analyzer were used for this purpose.

Mechanical behavior

The mechanical behavior of both the monolithic and composite samples was assessed using microhardness and tensile measurements. Microhardness was performed on the polished samples using a Matsuzawa MXT 50

automatic digital microhardness tester. The microhardness test was performed using a Vickers indenter under a test load of 25 gf and a dwell time of 15 s in accordance with the ASTM standard E384-99.

The tensile properties of the extruded monolithic magnesium and its composites were determined in accordance with ASTM standard E8M-01. The tensile tests were conducted on round tension test specimens of 5 mm in diameter and 25 mm gauge length using an automated servohydraulic testing machine (MTS 810) with a cross-head speed set at 0.254 mm/min. Fracture surface characterization studies were carried out on the tensile fractured Mg and $\text{Mg}/\text{Y}_2\text{O}_3$ samples to investigate the failure mechanisms using JEOL JSM-5600 LV scanning electron microscope.

Results

Macrostructure

The results of macrostructural characterization revealed that the outer surface of the compacted and sintered billets of both magnesium and magnesium nanocomposites showed no macroscopically observable signs of cracking and warping. After extrusion, the extruded rods were smooth and free of surface cracks except for the sample extruded at an extrusion ratio of 12:1 in which shallow circumferential cracks were observed in some portion of the rods.

Density measurements

The results of density and porosity measurements for pure magnesium and magnesium composite samples extruded at different extrusion ratios are shown in Fig. 1. The results revealed an increase in density, and therefore a decrease in porosity, with an increase in extrusion ratio for both monolithic and reinforced samples. The highest porosity, which is more than 1%, was observed in the composite sample extruded at the lowest extrusion ratio (12:1). In all cases, the porosity of the composite samples was higher than that of the equivalent monolithic samples (Fig. 1b).

Microstructural characterization

The results of grain morphology measurements for the samples extruded at different extrusion ratios are shown in Table 1 and Fig. 2. It was observed that the average grain size decreases with increasing extrusion ratio for both pure magnesium and the composite samples. As the extrusion ratio increases, the distribution of grain size also becomes more homogeneous for both monolithic and composite

Fig. 1 Effect of extrusion ratio on: (a) density and (b) porosity

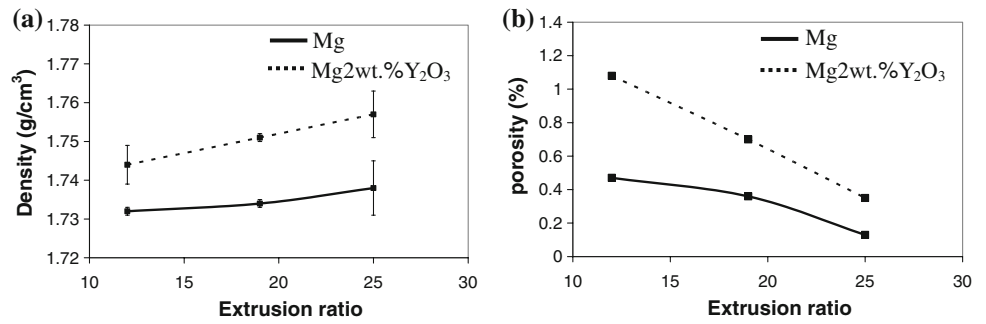


Table 1 Results of grain morphology determinations

Materials	Extrusion ratio	Grain characteristics	
		Size (µm)	Aspect ratio
Mg	12:1	37 ± 11	1.6 ± 0.4
Mg	19:1	31 ± 8	1.6 ± 0.3
Mg	25:1	20 ± 3	1.4 ± 0.1
Mg/2 wt.%Y ₂ O ₃	12:1	35 ± 9	1.6 ± 0.4
Mg/2 wt.%Y ₂ O ₃	19:1	28 ± 6	1.6 ± 0.3
Mg/2 wt.%Y ₂ O ₃	25:1	18 ± 3	1.4 ± 0.2

samples. This is evident from the reduction in standard deviations in the grain size of monolithic and composite samples. When the grain size of the pure magnesium is compared to that of magnesium nanocomposites extruded at different extrusion ratios, average grain size in the composite samples was smaller than that in the pure sample. Considering the standard deviation, the difference in grain size of monolithic and composite samples can be considered statistically insignificant. FESEM micrographs revealing the distribution of nano yttria particulates in magnesium matrix for the composite samples extruded

at different extrusion ratios are shown in Fig. 3. An improvement in uniformity of reinforcement particulate distribution with increasing extrusion ratio can be discerned. In the samples extruded at 12:1 extrusion ratio, yttria particulates were present mostly in clusters while in the samples extruded at 25:1 extrusion ratio, yttria particulates were present individually and in relatively smaller clusters indicating an improvement in their distribution (Fig. 3a and c).

Mechanical behavior

The results of microhardness measurements and room temperature tensile properties are shown in Figs. 4 and 5. It was observed that microhardness increases with an increase in extrusion ratio for both monolithic and composite samples (Fig. 4). In both samples, the microhardness increases only slightly when the extrusion ratio increases from 12:1 to 19:1, but shows a sharp rise when the extrusion ratio was increased to 25:1.

Results of room-temperature tensile testing revealed an increase in 0.2%YS and UTS with an increase in extrusion ratio for both monolithic and composite samples, again with the greatest increase occurring as the extrusion ratio

Fig. 2 Optical micrographs showing grain morphology of pure magnesium and magnesium nanocomposites extruded at different extrusion ratios

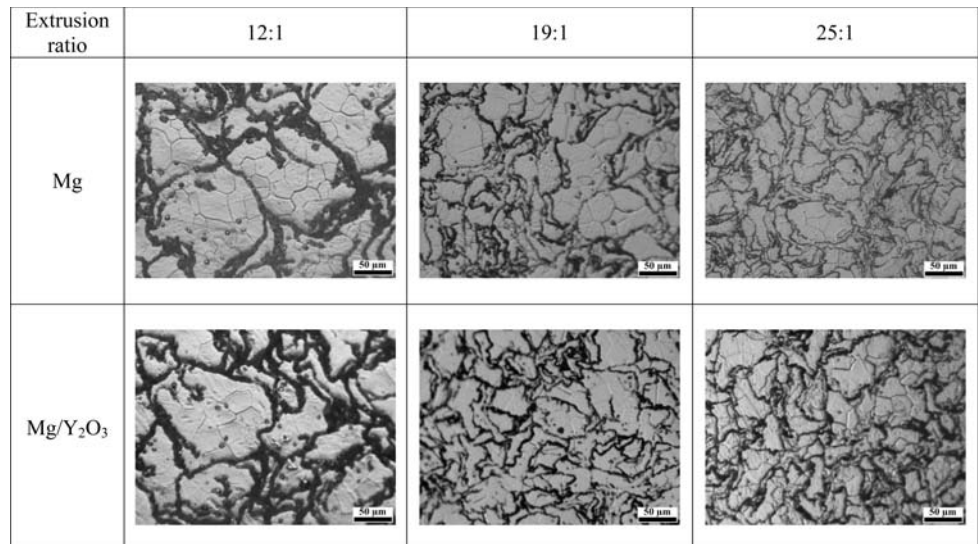


Fig. 3 FESEM micrographs showing particle distribution in Mg/Y₂O₃ nanocomposites extruded at extrusion ratio of (a) 12:1, (b) 19:1, and (c) 25:1

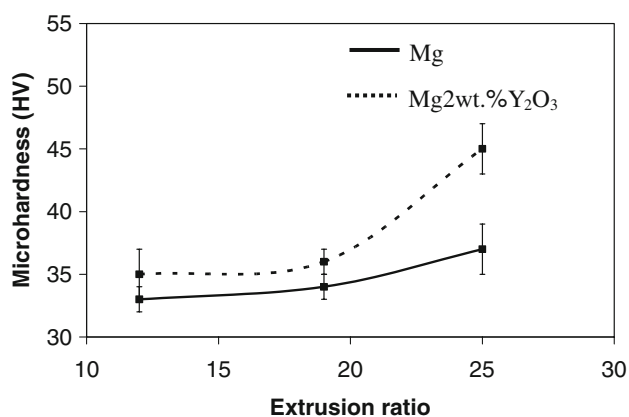
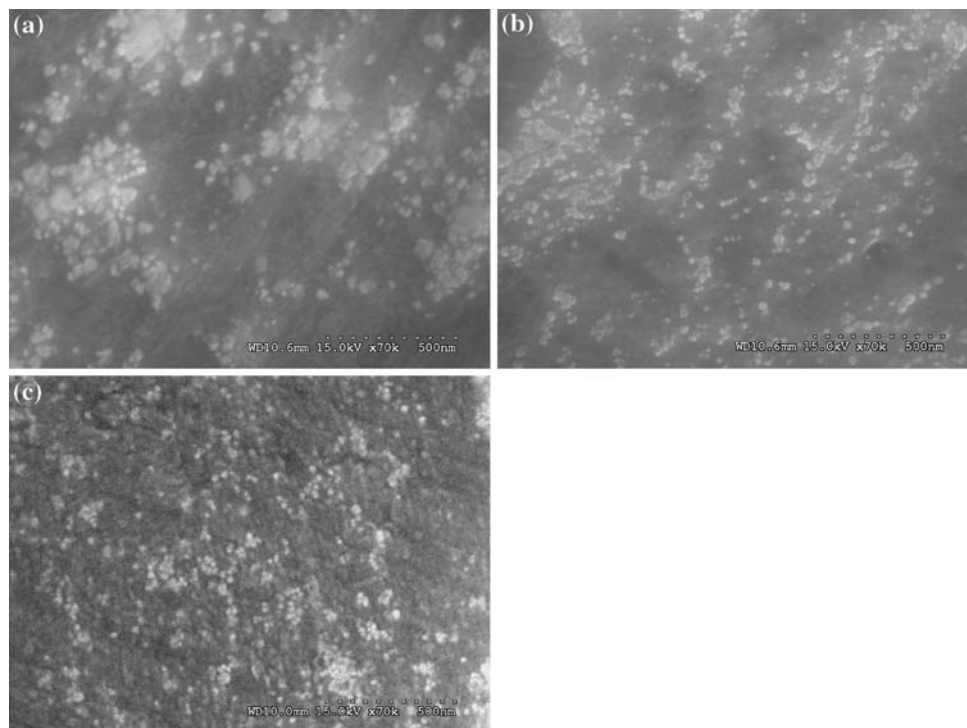


Fig. 4 Effect of extrusion ratio on microhardness

increased from 19:1 to 25:1. The ductility peaked at an extrusion ratio of 19:1 (Fig. 5). Results also revealed a significant increase in 0.2%YS and UTS of Mg/Y₂O₃ samples when the extrusion ratio was increased from 19:1 to 25:1. Significant decrease in ductility was observed in the case of pure magnesium, while the peak ductility value was maintained in the case of magnesium nanocomposite.

Fractography

Figure 6 shows the fractographs taken from the tensile fracture surfaces of pure magnesium and magnesium nanocomposites. In the case of pure magnesium, typical brittle fracture was observed in the sample extruded at the

highest extrusion ratio of 25:1 whereas some localized plastic deformation with formation of dimple-like features was observed in the samples extruded at lower extrusion ratios. In the case of composite samples, the fracture surfaces show evidence of plastic deformation, with the formation of dimple-like features in the samples extruded at higher extrusion ratios, while micron-size yttria particulate clusters were observed in the fracture surface of the sample extruded at lowest extrusion ratio (12:1).

Discussion

Densification behavior

The results from the current investigation, which show an increasing trend in density with increasing extrusion ratio for both pure magnesium and the magnesium nanocomposite samples, are reasonably in agreement with the previous study [17] in which an increase in density of glassy alloy compact with increasing extrusion ratio was reported. Lloyd reported that the use of high extrusion ratio could lead to more contact and good bonding between powder particles [1]. As the extrusion ratio increases, the degree of workability or deformability of the materials increases leading to an improvement in bonding between particles as a result of an increase in the extent of particle contact contributing to progressively higher density of samples. In accordance with the density results, the

Fig. 5 Effect of extrusion ratio on: (a) 0.2% yield strength, (b) ultimate tensile strength, and (c) failure strain

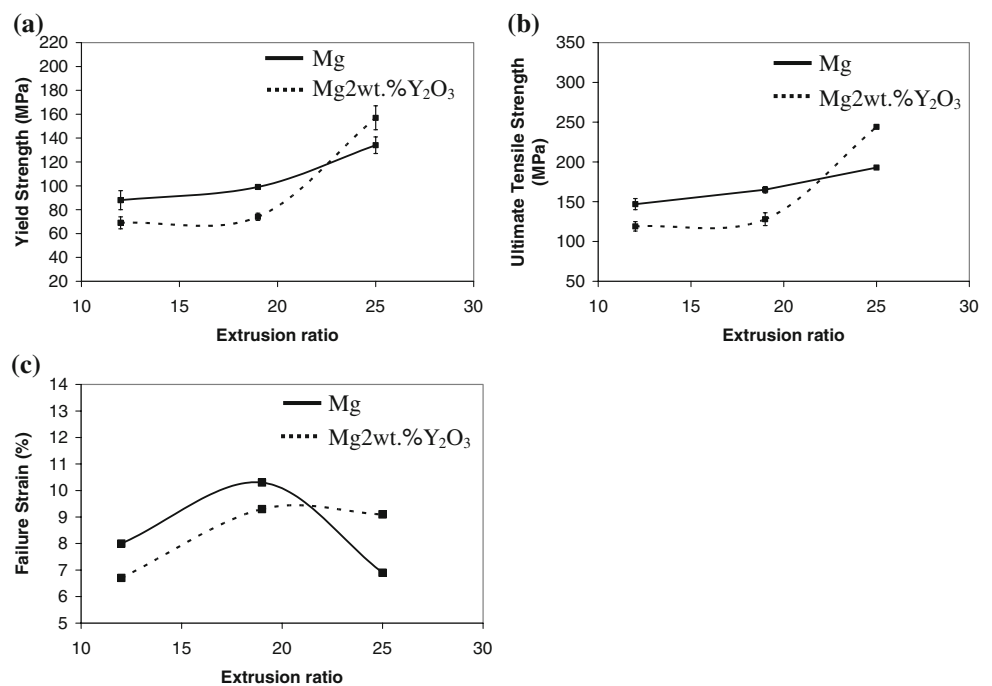
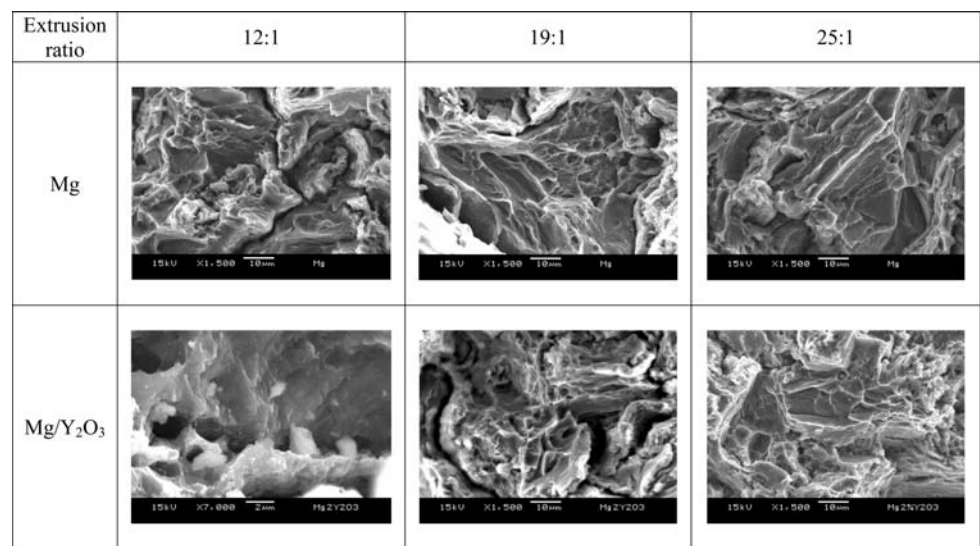


Fig. 6 Representative tensile fracture surfaces of pure magnesium and magnesium nanocomposites extruded at different extrusion ratios



porosity of samples decreased with increasing extrusion ratio. Although the decrease in porosity was steady in pure samples, a steep decrease in porosity was observed in composite samples with increasing extrusion ratio. This can be attributed to the breakdown of Y₂O₃ particulate clusters and a minimization of the particulate cluster-associated porosity (see Fig. 3) [1]. Presence of higher porosity in composite samples when compared to monolithic samples can be attributed to the presence of the particle and cluster-associated porosity. These findings are similar to the observations made on composites containing micron-size particulates [18, 19].

Microstructural evolution

Grain size determinations in monolithic and composite samples revealed the following:

- (a) Decrease in average grain size with an increase in extrusion ratio (Table 1 and Fig. 2).
- (b) Increase in homogeneity of grain size (Table 1).
- (c) Null effect of presence of nanoparticulates on grain size.

The decrease in grain size with increase in extrusion ratio can be attributed to an increased level of deformation,

and these results are consistent with the results obtained on AZ31 and AZ31B commercial magnesium alloys [13, 14]. Grain distribution curves shown in Fig. 7a and b also support the results shown in Table 1. The increase in homogeneity of grain size with an increase in extrusion ratio (smaller standard deviations for the mean grain size) indicates that the thermal exposure following the complete recrystallization of the matrix was limited, inhibiting the tendency for abnormal grain growth (Table 1).

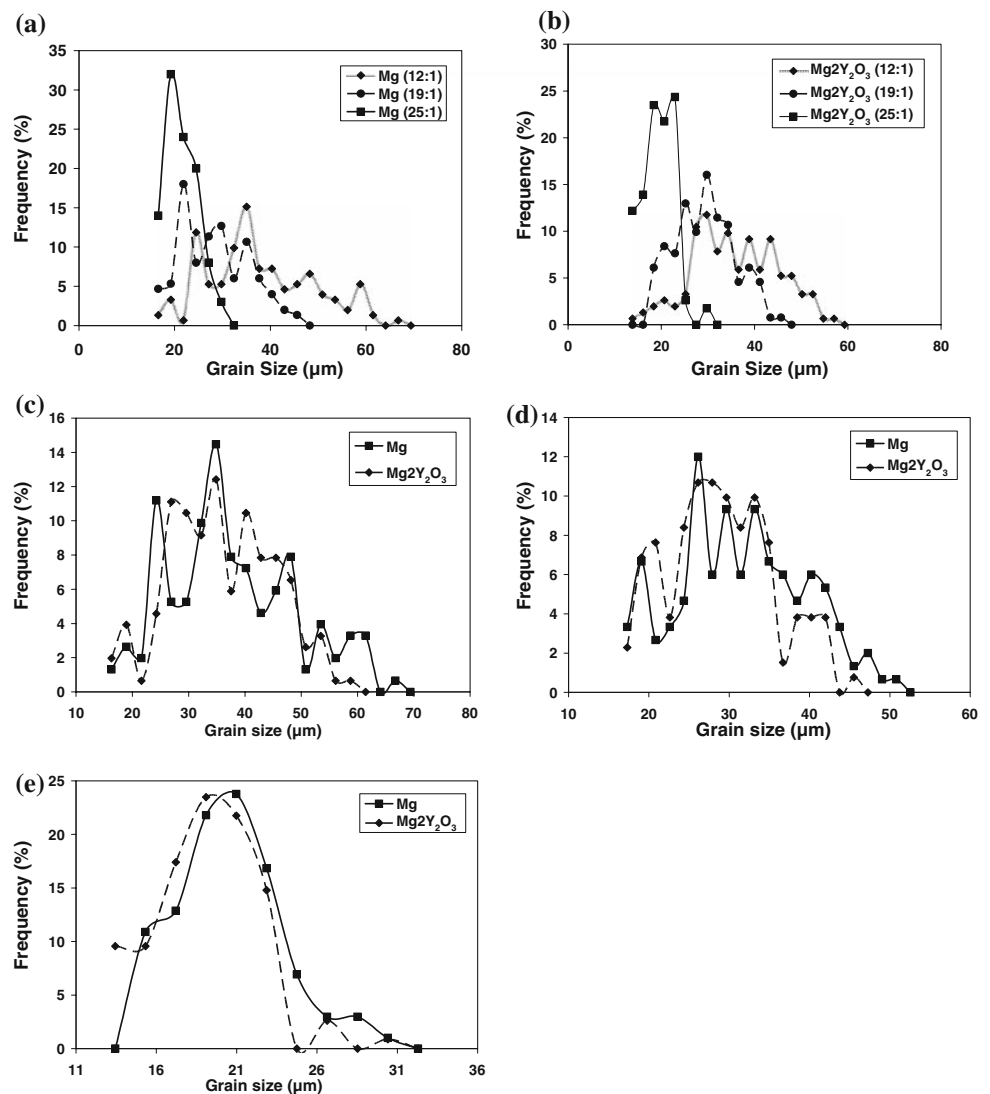
The null effect of yttria particulates on the grain size on a Mg matrix can be seen from Fig. 7c, d and e. Results clearly reveal that, unlike reinforcement particulates in micron length scale [20, 21], particulate-stimulated nucleation is not observed when the reinforcement particulates are in nano length scale [22, 23]. Similarly, the improvement in distribution with an increase in extrusion ratio (Fig. 3) can be attributed to an increase in the level of deformation during extrusion, leading to more shear

deformation and comparatively limited axial flow of composite matrix [24]. These results are consistent with the observations made earlier on the composites containing reinforcement particulates in micron length scale [1, 25].

Mechanical behavior

The results of microhardness measurements revealed that increasing the extrusion ratio leads to an increase in average microhardness of pure magnesium and magnesium nanocomposites. This can be attributed to: (a) improvement in distribution of Y_2O_3 particulates, (b) progressively decreasing average grain size (Table 1), and (c) reduction in the amount of porosity (Fig. 1) [26] with increasing extrusion ratio. The marginally higher microhardness of composite samples when compared to the monolithic samples at extrusion ratios of 12:1 and 19:1 can be attributed to the non-uniform presence of Y_2O_3 particulates

Fig. 7 Grain size distribution at different extrusion ratio for: (a) pure magnesium samples, (b) magnesium nanocomposite samples, and grain size distribution for pure magnesium and magnesium nanocomposite at extrusion ratio of: (c) 12:1, (d) 19:1, and (e) 25:1



while a significant increase in hardness at 25:1 extrusion ratio in case of Mg/Y₂O₃ composite can be attributed to the improved distribution of Y₂O₃ particulates. The results of microhardness measurements are consistent with results of microstructural characterization showing a clear improvement in the distribution of Y₂O₃ at 25:1 extrusion ratio (Fig. 3c). The increase in hardness with increasing extrusion ratio can partly be attributed to a reduction in grain size, however, the results revealed (Fig. 4) that a ~36% reduction in grain size in the case of pure Mg (from extrusion ratio 19:1 to 25:1) leads to only marginal improvement in hardness further suggesting the dominant role played by the distribution of reinforcement in improving the hardness in the case of composite samples.

It is well established that yield and tensile strengths normally increase with increasing extrusion ratio. Previous investigations on the effect of extrusion ratio on yield strength and/or ultimate tensile strength of aluminum alloys [27, 28], magnesium alloys [13–15], and magnesium alloy matrix composite [15] confirmed such a trend. The present study further confirms this trend for commercially pure magnesium and Mg/Y₂O₃ nanocomposite. The increase in yield and tensile strengths of monolithic and composite samples can be attributed to two common factors: (a) reduction in matrix grain size through classical Hall-Petch relationship and (b) decrease in amount of porosity with increasing extrusion ratio. Since the presence of pores, especially in powder-processed materials, can greatly influence the mechanical properties of materials [29], the use of an extrusion process with appropriately high extrusion ratios is very effective in reducing porosity content and thus realizing higher strength levels in materials. The degradation of strength due to increasing amount of porosity has been reported in the literature [18, 19, 29]. In addition, an increase in strengths of magnesium nanocomposites with increasing extrusion ratio can further be explained by the improvement in the distribution of yttria particulates in the magnesium matrix [15]. At extrusion ratios of 12:1 and 19:1, the strength values obtained in composite samples are similar and lower than those of the pure samples. The presence of the yttria particulates in magnesium matrix seems to degrade the properties of the composites because of the presence of particulate clusters, which remain due to the low extrusion ratio used (see Fig. 3a and b). When the extrusion ratio is increased from 19:1 to 25:1, both 0.2% YS and UTS increased significantly and exceeded that of pure Mg and this can be attributed primarily to the improvement in the distribution of Y₂O₃ particulates (Fig. 3c). This suggests that an extrusion ratio higher than a certain critical value is needed for efficient breakdown of particulate clusters particularly for powder-processed composite materials containing reinforcement in nano length scale.

Earlier investigations have revealed that in the case of magnesium alloys, an increase in extrusion ratio leads to an increase in ductility [13, 14]. In the present study, monolithic and composite samples showed an increase in ductility only when the extrusion ratio increases from 12:1 to 19:1. This increment in ductility may be attributed to the refinement in grain size [13, 14, 30] and low porosity percentage observed in the samples as extrusion ratio increases. The maximum ductility value was observed at critical extrusion ratio of 19:1 for both pure magnesium and nanocomposite samples. Especially for pure magnesium [31] and magnesium alloys [13, 14], the reduction in grain size is one of the most effective microstructural modification for improving both strength and ductility. However, a further increase in extrusion ratio from 19:1 to 25:1 led to a significant decrease in ductility of magnesium even though a finer grain and a lower porosity were achieved in the sample. A reduction in ductility with a decrease in grain size, resulting from increased plastic deformation in the equal-channel angular-pressed (ECAP) pure Mg was also observed in another study [32]. Kim [33] reported that a rapid material failure can occur due to the heterogeneity of void size even if the void volume fraction is low. This might be the cause of the low ductility with reduced porosity in pure magnesium in the current study. In the case of the composite sample, ductility remained similar when the extrusion ratio increased from 19:1 to 25:1 (Fig. 5c). The ductility of composite sample was higher than that of pure sample at extrusion ratio of 25:1. This may be attributed to the presence and homogenous distribution of nano particulates in magnesium matrix [1, 12, 34]. Furthermore, lower ductility values exhibited by composite samples when compared to pure sample at extrusion ratios of 12:1 and 19:1 can be attributed primarily to the presence of particulate-associated defects in the microstructure such as high porosity and formation of relatively large number of particulate clusters due to a relatively lower degree of plastic deformation at lower extrusion ratios [34].

The results of the present study also revealed an excellent agreement between microhardness and strength of pure magnesium and Mg/Y₂O₃ composite (see Fig. 8). The expressions with the degree of curve fit are shown below:

Pure Mg

$$YS = 11.538H - 293 \quad R^2 = 0.9999 \quad (1)$$

$$UTS = 11H - 213 \quad R^2 = 0.9758 \quad (2)$$

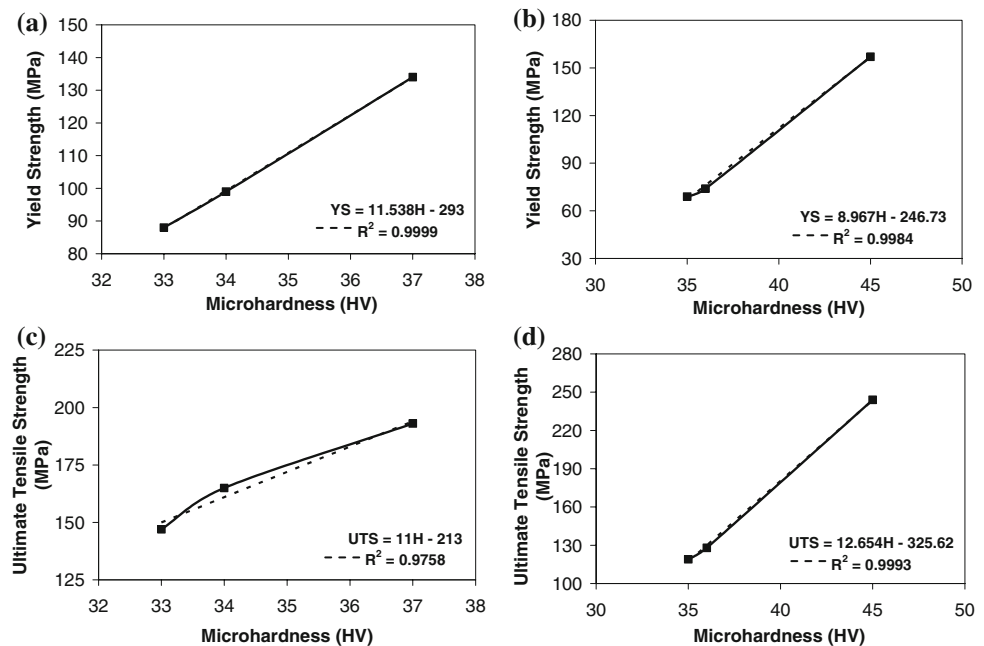
Mg/Y₂O₃

$$YS = 8.967H - 246.73 \quad R^2 = 0.9984 \quad (3)$$

$$UTS = 12.654H - 325.62 \quad R^2 = 0.9993 \quad (4)$$

where *H*, YS, and UTS represents microhardness, yield strength, and ultimate tensile strength, respectively. These near-perfect relationships suggest that for a given

Fig. 8 Relationship between microhardness and yield strength for: (a) Mg and (b) Mg/Y₂O₃ nanocomposite, and microhardness and ultimate tensile strength for: (c) Mg and (d) Mg/Y₂O₃ nanocomposite at different extrusion ratios



formulation the variation in processing can be assessed by hardness measurements which can be further correlated clearly with the tensile strengths.

Fractography

From the fractographic analysis, pure Mg extruded at an extrusion ratio of 25:1 fails predominantly in a brittle manner, showing the presence of cleavage steps. This is a common failure mode in hexagonally close-packed magnesium. For magnesium samples extruded at lower extrusion ratios, localized plastic deformation zones on the fracture surface of the sample were observed indicating a relatively more ductile mode of failure (Fig. 6). In the composite samples extruded at higher extrusion ratios of 19:1 and 25:1, observation of some plastic deformation in the tensile fractographs can be correlated with higher tensile ductility of the samples (Fig. 5). Both monolithic and composite samples extruded at 12:1 extrusion ratio showed the presence of cracks on fracture surface suggesting the presence of unacceptable porosity-related defects in the samples contributing to crack initiation and propagation at lower level of tensile plastic deformation.

Conclusions

1. Synthesis of monolithic Mg and Mg/Y₂O₃ nanocomposite can be successfully accomplished by using a microwave sintering approach followed by hot extrusion at different extrusion ratios.
2. An increase in extrusion ratio leads to an increase in density and reduction in porosity irrespective of the type of sample.

3. An increase in extrusion ratio leads to an improvement in homogeneity of microstructure in terms of grain morphology and reinforcement distribution. The best distribution of nano-size Y₂O₃ particulates was realized at an extrusion ratio of 25:1.
4. Microhardness and strengths for both samples increased with increasing extrusion ratio. The greatest increase in both hardness and strength occurred in composite sample when extrusion ratio was increased from 19:1 to 25:1. This increment is attributed to the homogenization in microstructure in terms of grain size and particulate distribution.
5. At critical extrusion ratio of 19:1, both pure and composite samples showed maximum ductility. Further increase in extrusion ratio was not effective for ductility enhancement.

Acknowledgement The authors wish to acknowledge NUS research scholarship for supporting the research effort.

References

1. Lloyd DJ (1994) *Int Mater Rev* 39:1
2. Evans A, Marchi CS, Mortensen A (2003) *Metal matrix composites in industry: an introduction and a survey*. Kluwer Academic, Dordrecht
3. Goh CS, Wei J, Lee LC, Gupta M (2007) *Acta Mater* 55:5115. doi:10.1016/j.actamat.2007.05.032
4. Hassan SF, Gupta M (2005) *Mater Sci Eng A* 392:163. doi:10.1016/j.msea.2004.09.047
5. Wong WLE, Gupta M (2007) *Compos Sci Technol* 67:1541. doi:10.1016/j.compscitech.2006.07.015
6. Perez P, Garces G, Adeva P (2004) *Compos Sci Technol* 64:145. doi:10.1016/S0266-3538(03)00215-X
7. Ferkel H, Mordike BL (2001) *Mater Sci Eng A* 298:193. doi:10.1016/S0921-5093(00)01283-1

8. Jiang QC, Wang HY, Ma BX, Wang Y, Zhao F (2005) *J Alloys Compd* 386:177. doi:[10.1016/j.jallcom.2004.06.015](https://doi.org/10.1016/j.jallcom.2004.06.015)
9. Wang HY, Jiang QC, Wang Y, Ma BX, Zhao F (2004) *Mater Lett* 58:3509. doi:[10.1016/j.matlet.2004.04.038](https://doi.org/10.1016/j.matlet.2004.04.038)
10. Graces G, Rodriguez M, Perez P, Adeva P (2006) *Mater Sci Eng A* 419:357. doi:[10.1016/j.msea.2006.01.026](https://doi.org/10.1016/j.msea.2006.01.026)
11. Xiuqing Z, Haowei W, Lihua L, Xinying T, Naiheng M (2005) *Mater Lett* 59:2105
12. Hassan SF, Gupta M (2007) *J Alloys Compd* 429:176. doi:[10.1016/j.jallcom.2006.04.033](https://doi.org/10.1016/j.jallcom.2006.04.033)
13. Chen Y, Wang Q, Peng J, Zhai C, Ding W (2007) *J Mater Process Technol* 182:281. doi:[10.1016/j.jmatprotec.2006.08.012](https://doi.org/10.1016/j.jmatprotec.2006.08.012)
14. Murai T, Matsuoka S, Miyamoto S, Oki Y (2003) *J Mater Process Technol* 141:207. doi:[10.1016/S0924-0136\(02\)01106-8](https://doi.org/10.1016/S0924-0136(02)01106-8)
15. Lee DM, Suh BK, Kim BG, Lee JS, Lee CH (1997) *Mater Sci Technol* 13:590
16. Gupta M, Wong WLE (2005) *Scripta Mater* 52:479. doi:[10.1016/j.scriptamat.2004.11.006](https://doi.org/10.1016/j.scriptamat.2004.11.006)
17. Kawamura Y, Kato H, Inoue A, Masumoto T (1996) *Mater Sci Eng A* 219:39. doi:[10.1016/S0921-5093\(96\)10437-8](https://doi.org/10.1016/S0921-5093(96)10437-8)
18. Cocen U, Onel K (2002) *Compos Sci Technol* 62:275. doi:[10.1016/S0266-3538\(01\)00198-1](https://doi.org/10.1016/S0266-3538(01)00198-1)
19. Tekmen C, Ozdemir I, Cocen U, Onel K (2003) *Mater Sci Eng A* 360:365. doi:[10.1016/S0921-5093\(03\)00461-1](https://doi.org/10.1016/S0921-5093(03)00461-1)
20. Inem B (1995) *Mater Sci Eng A* 197:91. doi:[10.1016/0921-5093\(94\)09753-4](https://doi.org/10.1016/0921-5093(94)09753-4)
21. Wang XJ, Wu K, Zhang HF, Huang WH, Chang H, Gan WM, Zheng MY, Peng DL (2007) *Mater Sci Eng A* 465:78. doi:[10.1016/j.msea.2007.03.077](https://doi.org/10.1016/j.msea.2007.03.077)
22. Doherty RD, Hughes DA, Humphreys FJ, Jonas JJ, Jensen DJ, Kassner ME, King WE, McNelley TR, McQueen HJ, Rollett AD (1997) *Mater Sci Eng A* 238:219. doi:[10.1016/S0921-5093\(97\)00424-3](https://doi.org/10.1016/S0921-5093(97)00424-3)
23. Shahani RA, Clyne TW (1991) *Mater Sci Eng A* 135:281. doi:[10.1016/0921-5093\(91\)90576-9](https://doi.org/10.1016/0921-5093(91)90576-9)
24. Gupta M, Sikand R, Gupta AK (1994) *Scripta Metal* 30:1343. doi:[10.1016/0956-716X\(94\)90270-4](https://doi.org/10.1016/0956-716X(94)90270-4)
25. Lloyd DJ, Lagace H, McLeod A, Morris PL (1989) *Mater Sci Eng A* 107:73. doi:[10.1016/0921-5093\(89\)90376-6](https://doi.org/10.1016/0921-5093(89)90376-6)
26. Bocchini GF (1986) *Int J Powder Metall* 22:185
27. Karabay S, Zeren M, Yilmaz M (2003) *J Mater Process Technol* 135:101. doi:[10.1016/S0924-0136\(02\)01110-X](https://doi.org/10.1016/S0924-0136(02)01110-X)
28. Karabay S, Yilmaz M, Zeren M (2005) *J Mater Process Technol* 160:138. doi:[10.1016/j.jmatprotec.2004.05.025](https://doi.org/10.1016/j.jmatprotec.2004.05.025)
29. German RM (1994) *Powder metallurgy science*, 2nd edn. Metal Powder Industries Federation, Princeton
30. Wang XL, Yu Y, Wang ED (2005) *Mater Sci Forum* 488–489:535
31. Robert CS (1960) *Magnesium and its alloys*. Wiley, New York
32. Yamashita A, Horita Z, Langdon TG (2001) *Mater Sci Eng A* 300:142. doi:[10.1016/S0921-5093\(00\)01660-9](https://doi.org/10.1016/S0921-5093(00)01660-9)
33. Kim TW (2006) *Scripta Mater* 55:1115. doi:[10.1016/j.scriptamat.2006.08.034](https://doi.org/10.1016/j.scriptamat.2006.08.034)
34. McDanel DL (1985) *Metall Trans A* 16A:1105. doi:[10.1007/BF02811679](https://doi.org/10.1007/BF02811679)